Expanding the Crystal Form Landscape of the Antiviral Drug Adefovir Dipivoxil

Rafel Prohens, [*,†] Rafael Barbas, [†] Anna Portell, [†] Mercè Font-Bardia, [‡] Xavier Alcobé, [‡] and Cristina Puigjaner [*,†]

†Unitat de Polimorfisme i Calorimetria, Centres Científics i Tecnològics, ‡Unitat de Difracció de Raigs X, Universitat de Barcelona, Baldiri Reixac 10, 08028 Barcelona, Spain

ABSTRACT

The solid state of adefovir dipivoxil (AD) has been revisited. In the present article we extend the knowledge about the solid state of this pharmaceutical prodrug. The stability landscape of the amorphous form with respect to the anhydrous and hydrate crystalline forms has been studied, and the use of an antiplasticizing agent to increase its Tg is described. The crystal structure of the elusive anhydrous form I has been determined from laboratory powder X-ray diffraction data by means of direct space methods using the computing program FOX. In addition, three new isostructural solvates of AD (methanol, ethylenglycol, and methylethylketone) have been discovered and structurally characterized by single crystal X-ray diffraction.

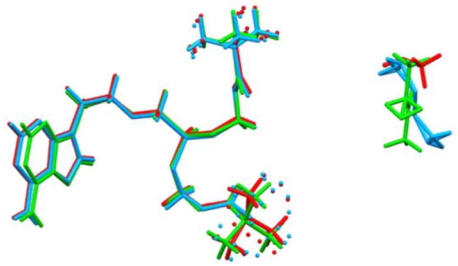

1. INTRODUCTION

The solid state properties of active pharmaceutical ingredients (APIs) are of great importance in the pharmaceutical field because the delivery of an API with the most suitable solubility, bioavailability and stability profiles depends on which crystal form of the drug is present. Most of the marketed drugs are polymorphic; thus the knowledge of the factors favoring a particular crystal form can be vital during the development of a pharmaceutical formulation.1

Adefovir dipivoxil (9-{2-[bis(pivaloyloxymethoxy)- phosphinylmethoxy]ethyl}adenine, AD hereafter) (Figure 1) is a nucleotide reverse transcriptase inhibitor that exhibits a marked in vivo antiviral activity against both HIV and HBV,2,3 and it is effective against other several human virus. In particular, AD is an important drug for the treatment of hepatitis B virus infection.4−6

The relevance of this drug has prompted in the past an intensive solid state research, resulting in a high number of crystal forms. The AD solid state forms that have been reported in the literature include the amorphous,7 three anhydrous polymorphs,8−10 a dihydrate,11 two polymorphic monohydrates, 12 a hemihydrate,13 a methanol solvate,8 a butanolate solvate,14 a novel crystal form with 6.0%−7.5% water content,15 a dichloromethane hemi solvate and another anhydrous form,16 and several salts and cocrystals.17 Moreover, different local patents describe other forms.18,19 Although five multicomponent crystal structures have been described in the literature (a succinic acid cocrystal,20 a saccharin cocrystal,21 a suberic acid cocrystal,20 a nicotinamide cocrystal,17 and a dihydrate11), the crystal structure of any anhydrous form remains, so far, elusive.

Hence, with the aim of extending the solid state knowledge of AD we are reporting for the first time the crystal structure of the anhydrous form I together with three new isostructural solvate forms. Moreover, the relative stability among the polymorphs and amorphous phases is described, and the use of an antiplasticizing agent to stabilize the amorphous AD is investigated.

2. MATERIALS AND METHODS

2.1. Synthesis of the Different Crystal Forms.

2.1.1. Form I. It was obtained by slow crystallization from a solution of AD in anhydrous MEK, AcOEt, toluene, heptane, xylene, or MTBE. (mp 98 °C).

2.1.2. Form II. It was obtained from a methodology described in the literature:4 N,N′-dicyclohexyl-4-morpholinecarboxamidine and chloromethyl pivalate were added to a solution of 9-[2-(phosphonomethoxy)ethyl]adenine in anhydrous DMF. After 36 h of stirring at room temperature, the insolubles were filtered off, and the filtrate was concentrated in vacuo, and it was purified by silica gel chromatography (mp 78 °C).

2.1.3. Form III. It was obtained by precipitation after the addition of pentane to a solution of AD in heptane (mp 93 °C).

2.1.4. Form IV. It was obtained by slow crystallization from a solution of 50 mg of AD in THF (mp 80 °C).

2.1.5. Form V. It was obtained by slow crystallization from a solution of 100 mg of AD in dichloromethane (mp 91 °C).

2.1.6. Dihydrate. It was obtained by crystallization at low temperature from not anhydrous MEK, THF, MIBK, AcOEt, or H2O (TGA analysis shows a weight loss of 6.9% which corresponds to two molecules of water).

2.1.7. Methanol Solvate. It was obtained by precipitation of a dissolution of AD in methanol at 0 °C (TGA analysis shows a weight loss of 6% which suggests a 1:1 stoichiometry).

2.1.8. Ethylenglycol Hemisolvate. It was obtained from precipitation of a dissolution of AD in ethylenglycol at −10 °C (TGA analysis shows a weight loss of 5.9% which suggests a 2:1 (AD/ethylenglycol) stoichiometry).

2.1.9. Methylethylketone Hemisolvate. It was obtained by evaporation at r.t. of a solution of AD in MEK (TGA analysis shows a weight loss of 4.7% which suggests a 2:1 (AD:MEK) stoichiometry).

2.1.10. Preparation of 1:3 AD-Copovidone Solid Dispersion. AD (60 mg) and copovidone (180 mg) were dissolved in 5 mL of dioxane at r.t. The solution was frozen at −40 °C (acetone/CO2), and it was lyophilized during 2 h until dryness. An amorphous white solid was obtained (Tg 71 °C, 100% yield).

2.2. Methods. 2.2.1. Powder X-ray Diffraction (PXRD). Powder X-ray diffraction patterns were obtained on a PANalytical X'Pert PRO MPD diffractometer in transmission configuration using Cu Kα1 + 2 radiation (λ = 1.5418 Å) with a focalizing elliptic mirror, a PIXcel detector working at a maximum detector's active length of 3.347°. Capillary geometry has been used with samples placed in glass capillaries (Lindemman) of 0.5 mm of diameter measuring from 2 to 60° in 2θ, with a step size of 0.026° and a total measuring time of 30 min. Flat geometry has been used for routine samples sandwiched between low absorbing films (polyester of 3.6 μm of thickness) measuring 2θ/θ scans from 2 to 40° in 2θ with a step size of 0.026° and a measuring time of 76 s per step. Powder X-ray diffraction pattern of form I was obtained using capillary geometry and soller slit of 0.01 radians. The sample was placed in a capillary of 0.7 mm and consecutive 2θ scans from 2 to 70° were measured and added. The total measuring time was 60 h.

2.2.2. Single Crystal X-ray Diffraction. MAR345 diffractometer with an image plate detector was used. Intensities were collected with graphite monochromatized MoKα radiation (λ = 0.71073 Å) using a

ϕ−scan technique. The structures were solved by direct methods using SHELXS computer program22 and refined by full-matrix least-squares method with SHELX97 computer program.

2.2.3. Differential Scanning Calorimetry (DSC). Differential scanning calorimetry was carried out by means of a Mettler-Toledo DSC-822e calorimeter or a Mettler-Toledo DSC30 calorimeter. Experimental conditions: aluminum crucibles of 40 µL volume or light aluminum pans of 20 µL volume, atmosphere of dry nitrogen or helium with 50 mL/min flow rate, heating rate of 10 °C/min and 100 °C/min. Both calorimeters were calibrated with indium of 99.99% purity.

2.2.4. Thermogravimetric Analysis (TGA). Thermogravimetric analyses were performed on a Mettler-Toledo TGA- 851e thermobalance. Experimental conditions: alumina crucibles of 70 µL volume, atmosphere of dry nitrogen with 50 mL/min flow rate, heating rate of 10 °C/min.

3. RESULTS AND DISCUSSION

3.1. Amorphous Form of AD. AD is reported to be obtained as an amorphous solid during the synthetic process,7 and many local patents describe its preparation.23−25 Therefore, we started the present work by studying the amorphous form of AD. All the attempts of preparation of the amorphous solid (lyophilization, quick evaporation, and cooling of saturated solutions) were unsuccessful, yielding mixtures of crystalline/amorphous solids. It is well recognized that amorphous phases are relatively reactive and can undergo significant changes even when stored in an inert environment.26 For example, they can absorb water very quickly when exposed to ambient conditions for a short period of time.

The aforementioned problems can be circumvented by preparing the amorphous phases and characterizing them without exposure to ambient conditions. One possible approach is to prepare the amorphous phase in situ, in the sample chamber of the instrument used for its characterization. This process will provide complete control, not only over the method of preparation, but also over the subsequent storage conditions of the prepared amorphous phase. Thus, the sample history will be completely known.

So, we decided to prepare the amorphous form in situ into the sample chamber of a differential scanning calorimeter (DSC) under nitrogen purge. After melting AD, the quenching from the melt resulted in the formation of the amorphous form, which was immediately characterized in the instrument without exposure to ambient environment. While amorphous phase was being heated, three thermal events were observed (Figure 2). Initial heating resulted in a change in the heat capacity at 12 °C (ΔCp= 0.963 J/gK) with no heat absorbed or evolved, attributed to a glass transition (Tg) to a supercooled liquid phase. The resulting unstable supercooled liquid crystallizes spontaneously upon heating at 71 °C. Further heating results in the melting at 78 °C of the crystalline form obtained.

The stability of this amorphous phase has also been studied. Amorphous solids are characterized by the glass transition, the temperature at which they transform from a glassy state to a rubbery material. The molecular mobility increases in the rubbery state, and rapid crystallization can occur above Tg. If Tg is below room temperature, as is the case under study, the amorphous state will be metastable at room temperature, and it will be very difficult to isolate. These data explain our unsuccessful attempts of preparation of the amorphous phase, where mixtures of amorphous and crystalline forms were always obtained. On the other hand, the Tg/Tm value of 0.77 for AD falls in the typical reported 0.69−0.85 range27 for most of glassy pharmaceuticals.

We also characterized the amorphous form of AD by means of powder X-ray diffraction (PXRD), by preparing a sample in a 0.5 mm capillary tube under argon atmosphere, heating it upon the melting temperature, and rapidly cooling it to −65 °C. PXRD permitted us to monitor the transformation of the amorphous AD into the crystalline form as a function of time. The PXRD pattern of this sample recorded at room temperature reveals the diffuse halos characteristic of amorphous phases. Different PXRD patterns were collected periodically (Figure 3), and after some hours peaks due to crystalline AD progressively increased.

Crystallization appeared to be completed in some days. Interestingly, the crystalline form observed after 2 days (form II) also transformed completely into a different polymorph (form I) after 12 days. Hence, PXRD analysis led to the conclusion that amorphous AD obtained in situ after quenching the melt transforms into a metaestable form II, which eventually transforms into the most stable form I, according to the Ostwald's so-called "Rule of Stages".28 On the other hand, it was also observed that amorphous AD transformed into the known dihydrate when exposed to air atmosphere.

All these data demonstrate that amorphous AD is not suitable for solid formulations due to its low stability at room temperature. However, if the time scale of devitrification was large (several years), then

recrystallization from the amorphous state could be considered irrelevant. In this sense, the glass transition temperature is a key parameter that indicates a borderline between high and low molecular mobility of a drug, and it has been shown that the molecular mobility becomes insignificant with respect to the shelf life stability at 50 K below Tg.29 Amorphous drugs having a low Tg value can benefit from protection from recrystallization using an antiplasticizing agent to increase the Tg. Therefore, crystallization of the amorphous can be inhibited by increasing the glass transition temperature of a solid dispersion by the addition of a polymer excipient with a high Tg. 30 This stabilization can be due not only to the antiplasticizing effect of the polymer but also to the intermolecular interactions between drug and polymer. The antiplasticizing effect of the polymer on drugs in solid dispersions has been studied for some active pharmaceutical ingredients, by analyzing the Tg variation as a function of the polymer concentration.31 The Gordon−Taylor32 eq 1 for binary mixtures allows predicting the Tg value.

$$T_g = \frac{w_1 T_{g1} + K w_2 T_{g2}}{w_1 + K w_2} \quad (1)$$

where w1 and w2 are the weight fractions of the drug and the polymer respectively, and Tg1 and Tg2 are the glass transition temperatures of both components. K can be calculated through eq 2, where ρ1 is the density of the amorphous drug and ρ2 is the density of the polymer.

$$K = \rho_1 T_{g1} / \rho_2 T_{g2} \quad (2)$$

In the present case, we explored the possibility of stabilizing the amorphous AD by preparing a solid dispersion with Copovidone as the antiplasticizing polymer. Copovidone is a 60:40 linear random copolymer of 1-vinyl-2-pyrrolidone and vinyl acetate with a reported Tg value of 105 °C.33 Therefore, some dioxane solutions of AD and copovidone in different proportions (AD/copovidone 1:1, 1:3, 2:1, and 3:1 in weight) were frozen to −40 °C and lyophilized. Amorphous solids were obtained from 1:1 and 1:3 solid dispersions, whereas mixtures of form II and amorphous were obtained from 2:1 and 3:1 solid dispersions (Figure 4).

The 1:1 solid dispersion was not stable at r.t. as partial crystallization to form II was observed after 1 week. Therefore, the selected candidate was the 1:3 AD/copovidone solid dispersion which showed a glass transition value of 71 °C when analyzed by DSC (Figure 5), which is lower than the predicted Tg value of 96 °C by the Gordon−Taylor model.

The stability of the 1:3 solid dispersion was studied under different storage conditions. The solid dispersion remained in the amorphous state at least for three months at 5 °C, r.t and 50 °C. Some crystallization traces of form I and AD dehydrate were observed after 1 week at 75% RH. These observations confirm that crystallization of AD is effectively inhibited by the combination with copovidone, being the 1:3 AD/copovidone the most stable combination. However, this solid dispersion should be kept under anhydrous conditions in order to prevent its crystallization.

3.2. Solid Forms Screening. Bearing in mind the two forms identified when studying the stability of the amorphous phase, we conducted a polymorph screening of AD in order to obtain and characterize as many forms as possible. Using a broad set of thermodynamic and kinetic crystallization conditions from a variety of solvents, we were able to isolate five different anhydrous crystalline forms (I, II, III, IV, and V), the dihydrate, the methanol solvate, and the ethylenglycol and MEK hemisolvates. A summary of all experimental conditions can be found in Supporting Information. All forms were characterized by means of PXRD, DSC, and TGA. Among all these solid forms, polymorphs IV and V and ethylenglycol

and MEK hemisolvates were not previously reported, whereas form I corresponds to the form 1 reported by Gilead Sciences,8 form II had been previously reported in CN101054393,9 and form III corresponds to the crystal form reported in US2006025384.10 Regarding the solvates, the dihydrate and the methanol solvate correspond to forms 2 and 3, respectively, reported by Gilead Sciences.8

The powder X-ray diffractograms of the different anhydrous forms and the solvates are shown in Figures 6 and 7 respectively, while Figure 8 shows the DSC of the different anhydrous forms. TGA analysis of these forms shows no weight loss from r.t. to 150 °C (data not shown).

It is of practical interest to know the relative thermodynamic stability of the anhydrous forms, and the main questions to solve are (i) to determine the most stable form at r.t. and (ii) whether two polymorphs are monotropically (one form is more stable than the other at any temperature) or enantiotropically (a transition temperature exists, below and above which the stability order is reversed) related, and for an enantiotropic system, where the transition temperature lies. Thermal analysis provides information about the melting temperature and the enthalpy of fusion of each form, which can be useful in defining the relative stability among all the forms. According to the Heat of Fusion Rule by Burger and Ramberger,34 forms I and II are monotropically related since the highest melting form I has the highest enthalpy of fusion. Thus, form I is thermodynamically more stable than form II at all temperatures up to the melting point. This fact is in agreement with the mentioned observation that amorphous AD transforms into form II which finally transforms into form I.

However, as can be seen in Figure 8, forms III, IV, and V do not show a single melting endotherm but additional phenomena such as crystallization from the melt and subsequent melting. In order to prevent these additional phenomena, DSC analysis were performed at high heating rate (100 °C/min), under helium atmosphere and using light aluminum pans to improve resolution. Table 1 summarizes the physicochemical data obtained for the anhydrous modifications of AD.

Regarding the stability among all anhydrous forms, although some of the polymorphs show very similar melting points, it can be suggested that all forms are monotropically related (since in each pair of forms the highest melting form has always the highest enthalpy) and with the following order of stability: form I > form III > form V > form IV > form II.

Commonly, the most stable polymorphic modification is used in a marketed formulation because any other polymorphs are metastable and may therefore transform into the most stable form. Overlooking the most stable polymorph may cause failure of a marketed product because a phase transformation during storage can occur. A late-appearing stable polymorph can have a great impact on development timelines35 as has been shown by many reviews written on disappearing polymorphs.36 However, metastable forms may survive years if a high activation energy barrier has to be overcome in moving from the metastable form to the stable one. In the present case, some information about the stability of the different anhydrous forms of AD has been obtained under three different conditions: r.t., 50 °C and r.t./75% RH. Form I has shown to be stable after one month of storage at r.t. and after 1 week of storage at 50 °C. However, when leaving form I 1 week in a desiccator at 75% RH, it transforms partially to the dihydrate. Forms II and IV have resulted to be stable after 1 month at r.t, but they transform to form I at 50 °C and to the dihydrate if they are exposed to 75% relative humidity conditions. Form III is stable after at least 2 weeks at r.t. and form V has shown to be stable at r.t. after one month but it transforms also to the dihydrate at r.t./75% RH.

3.3. Crystal Structures Analysis. 3.3.1. Form I of Adefovir Dipivoxil. Attempts to grow quality crystals of AD form I were unsuccessful. Thus, the resolution of its crystal structure was attempted using the direct space methodology. The indexation of its monoclinic Cc cell was performed using Dicvol04.37 The final refined cell parameters are a = 13.1287(1) Å, b = 24.6784(3) Å, c = 8.34752(8) Å, β = 100.6575(5)°; V = 2657.90(5) Å3, Z = 4 with one molecule in the asymmetric unit. The crystal structure was solved by means of direct space methods using the program FOX38 with the parallel

tempering algorithm. In order to accelerate the process during the parallel tempering calculation, the powder pattern was truncated to $2\theta = 35°$ (CuKα1). The starting model of 1 was previously optimized with the commercial program SPARTAN, and some constraints were introduced to FOX, considering aromatic rings as rigid groups. Several trials of 20 million runs were performed. Subsequently the structure was refined by the Rietveld method with FullProf.39 Figure 9 depicts the final Rietveld plot.

Form I crystallizes with one molecule of AD in the asymmetric unit (Figure 10) forming ribbons linked through hydrogen-bonded adenine moieties. Both Watson−Crick and Hoogsteen modes of interaction between adenine units are involved in the hydrogen-bonding assembly (Figure 12). The ribbon arrangement has been observed commonly in nucleobase pairs; however, ribbons formed only by adenine molecules were only observed for the first time in an adenine/ metal carboxylate complex40 and a similar ribbon motif has been observed in the structure of 9-methyladenine.41

3.3.2. Isostructural Solvates. Three solvates have been identified and their crystal structures were solved by means of single crystal X-ray diffraction. The three solvates constitute a family of isostructural solvates with the solvent molecules (MeOH, ethylenglycol, and MEK) residing in similar regions of the crystal structure. This phenomenon has been observed previously for a variety of pharmaceutical compounds such as Finasteride,42 Tenofovir disoproxyl fumarate,43 olanzapine,44 and Nevirapine.45 The three triclinic structures crystallize in the $P\bar{1}$space group with very similar unit cell parameters (Table 2). Figure 11 displays the overlapped asymmetric unit for the three solvates. In the MEK and ethylenglycol hemisolvates, the solvent molecules are disordered around an inversion center.

The main intermolecular interactions are common; Hoogsteen pairing of adenine moieties in combination with strong PO···HN contacts which form the backbone of the crystal structure are reinforced by weaker secondary interactions as shown in Figure 12. In the case of the methanol and ethylenglycol solvates, the solvent molecule establishes a strong hydrogen bond with the pyperidine nitrogen, while in the MEK hemisolvate although the solvent molecule occupy the same position, only weak CO···HC contacts are formed. On the other side, the previously published dihydrate structure11 presents the same Hoogsteen pairing motif, while water molecules establish hydrogen bonds with the pyperidine nitrogen and the NH2 group of the adenine moiety. However, it is not isostructural to the three solvates presented in this work.

Finally, some cocrystal forms with carboxylic acids have been reported and crystal structures with the succinic46 and suberic acids47 have been solved. The succinic acid cocrystal (the only one available at the CCDC) shows complementary hydrogen bonded assemblies of adenine/carboxylic acid interactions which break the adenine self-assembling motif. This R2 2(9) heterosynthon is evidence of hydrogen bonding in the Hoogsteen mode.48

4. CONCLUSION

The present study focused on extending the solid state landscape of the important prodrug Adefovir dipivoxil. Two new polymorphs and two new solvates of Adefovir dipivoxil have been identified during an intensive solid forms screening. The stability of the amorphous phase has been studied, and the use of copovidone as antiplasticizing agent has shown to inhibit its crystallization under anhydrous conditions. Moreover, the interconversion among all the known crystal forms has been investigated, being the most stable form I monotropically related with the rest of the anhydrous forms. The elusive crystal structure of form I has been determined by means of direct space methods, while the crystal structures of three solvates have been solved from single crystal X-ray diffraction. Data have shown that these solvates are metrically isostructural (very similar unit cell and the same space group), and the analysis of the crystal structures revealed important differences in the intermolecular interactions with respect to those in form I.

AUTHOR INFORMATION

Corresponding Authors

*(R.P.) Tel. + 34 93 4034656. Fax. + 34 93 4037206. E-mail: rafel@ccit.ub.edu.
*(C.P.) E-mail: cris@ccit.ub.edu.

Notes

The authors declare no competing financial interest

REFERENCES

(1) Bernstein, J. Cryst. Growth Des. 2011, 11, 632−650.

(2) De Clercq, E. Biochem. Pharmacol. 1991, 42, 963−972.

(3) Heijtink, R. A.; De Wilde, G. A.; Kruining, J.; Berk, L.; Balzarini, J.; De Clercq, E.; Holý, A.; Schalm, S. W. Antiviral Res. 1993, 21, 141−153.

(4) Julander, J. G.; Sidwell, R. W.; Morrey, J. D. Antiviral Res. 2002, 55, 27−40.

(5) Qaqish, R. B.; Mattes, K. A.; Ritchie, D. J. Clin. Ther. 2003, 25, 3084−3099.

(6) Hadziyannis, S. J.; Papatheodoridis, G. V. Expert. Rev. Anti. Infect. Ther. 2004, 2 (4), 475−83.

(7) Starrett, J. E.; Tortolani, D. R.; Rusell, J.; Hitchcock, M. J. M.; Whiterock, V.; Martin, J. C.; Mansuri, M. M. J. Med. Chem. 1994, 37, 1857−1864.

(8) Arimilli, M. N.; Lee, T. T. K.; Manes, L. V.; Munger, J. D.; Prisbe, E. J.; Schultze, L. M.; Kelly, D. E. Nucleotide analog compositions. WO 99/047741999.

(9) CN2006/101054393A.

(10) Wang, G.; Lu, X.; Liu, Q.; Tang, Y.; Yang, L.; New crystal form of adefovir dipivoxil and its composition. US2006/0025384A1, 2006.

(11) Chang, Y.; Zheng, Q.; Lu, Y. Acta Crystallogr. Sect. E 2007, E63, o1014−o1015.

(12) Galimi, S.; Vecchio, E.; Pizzocaro, R. Adefovir dipivoxil crystalline monohydrate form. WO 2009/015892A1, 2009.

(13) Ahn, J. H.; Kim, U. S.; Choi, A. R. Preparation of adefovir dipivoxil hemihydrate. KR 2011024354A, 2011.

(14) Oh, H. S.; Byun, E. Y.; Jang, S. M.; Ha, T. H.; Kim, H. K.; Suh, K. H.; Lee, G. S. Method for preparing crystalline adefovir dipivoxil and adefovir dipivoxil butanolate used therein. WO2010/120074A2, 2010.

(15) Parthasaradhi, B.; Rathnakar, K.; Raji, R.; Muralidhara, D.; Madhan, M.; Vamsi, B.; Sridhar, D. Novel polymorphs of adefovir dipivoxil. WO 2011/016044A1, 2011.

(16) An, J.; Choi, G. J.; Kim, W. Int. J. Pharm. 2012, 422, 185−193.

(17) Blazecka, P. G.; Che, D.; McPhail, C. L. Rey, A. W.; Salt form and cocrystals of adefovir dipivoxil and processes for preparation thereof. US 2009/0247749A1, 2009.

(18) Huaming, Z.; Ying, Z.; Aiming, W.; Fei, L. New crystal form of adefovir dipivoxil for pharmaceuticals. CN1425673A, 2003.

(19) Dianzhen, Z.; Li, Z.; Jian, Z.; Jianqiang, Z.; Wulin, L.; Yabo, D.; Minghua, Z. New crystal form of adefovir dipivoxil and its preparation. CN 1435420A, 2003.

(20) Jung, S.; Lee, J.; Kim, I. W. J. Cryst. Growth 2013, 373, 59−63.

(21) Gao, Y.; Zu, H.; Zhang, J. J. Pharm. Pharmacol. 2011, 63, 483−490.

(22) Sheldrick, G. M., SHELXS: A Program for Automatic Solution of Crystal Structure; University of Göttingen: Göttingen: Germany, 1997.

(23) Lei, Z.; Hui, L.; Wenji, X. Preparation of amorphous adefovir dipivoxil solid. CN 1374314A, 2002.

(24) Ye, J.; Lijuan, K.; Lifang, Z. Method for preparation of amorphous adefovir dipivoxil. CN 1670025A, 2005.

(25) Peiling, C.; Xiaorong, S. Amorphous adefovir dipivoxil solid dispersion type oral preparation and preparation method thereof. CN 102920673A, 2013.

(26) Li, Y.; Han, J.; Zhang, G. G. Z.; Grant, D. J. W.; Suryanarayanan, R. Pharm. Dev. Technol. 2000, 5 (2), 257−266.

(27) Fukuoka, E.; Makita, M.; Nakamura, Y. Chem. Pharm. Bull. 1991, 39 (8), 2087−2090.

(28) Bernstein, J. Polymorphism in Molecular Crystals; Clarendon Press: Oxford, 2002.

(29) Hancock, B. C.; Shamblin, S. L.; Zografi, G. Pharm. Res. 1995, 12, 799−806.

(30) Miyazaki, T.; Yoshioka, S.; Aso, Y. Chem. Pharm. Bull. 2006, 8, 1207−1210.

(31) Van der Mooter, G.; Wuyts, M.; Blaton, N.; Busson, R.; Grobet, P.; Augustijns, P.; Kinget, R. Eur. J. Pharm. Sci. 2001, 12, 261−269.

(32) Gordon, M.; Taylor, J. S. J. Appl. Chem. 1952, 2, 493−501.

(33) Gupta, S. S.; Meena, A.; Parikh, T.; Serajuddin, A. T. M. J. xcipients Food Chem. 2014, 5 (1), 32−45.

(34) Burger, A.; Ramberger, R. Mikrochim. Acta I 1979, 259.

(35) Desikan, S.; Parsons, R. L.; Davis, W. P.; Ward, J. E.; Marshall, W. J.; Toma, P. H. Org. Process. Res. Dev. 2005, 9, 933.

(36) Llinas, A.; Goodman, J. Drug Discovery Today 2008, 13, 198−210.

(37) Boultif, A.; Louër, D. J. Appl. Crystallogr. 2004, 37, 724.

(38) Favre-Nicolin, V.; Czerny, R. J. Appl. Crystallogr. 2002, 35, 734−743.

(39) Rodríguez-Carvajal, J. Physica B 1993, 192, 55−69.

(40) Dobrzynska, D.; Jerzykiewicz, L. B. J. Am. Chem. Soc. 2004, 126, 11118−11119.

(41) King, M. D.; Ouellette, W.; Korter, T. M. J. Phys. Chem. A 2011, 115, 9467−9478.

(42) Schultheiss, N.; Smit, J. P.; Hanko, J. A. Eur. J. Pharm. Sci. 2009, 38, 498−503.

(43) Lee, J.; Boerrigter, S. X. M.; Jung, Y. W.; Byun, Y.; Yuk, S. H.; Byrn, S. R.; Lee, E. H. Eur. J. Pharm. Sci. 2013, 50 (3−4), 253−262.

(44) Thakuria, R.; Nangia, A. Cryst. Growth Des. 2013, 13 (8), 3672−3680.

(45) Stieger, N.; Liebenberg, W.; Wessels, J. C.; Samsodien, H.; Caira, M. R. Struct. Chem. 2010, 21 (4), 771−777.

(46) Jung, S.; Ha, J. M.; Kim, I. W. Acta Crystallogr. 2012, E68, o809−o810.

(47) Jung, S.; Lee, J.; Kim, I. W. J. Cryst. Growth 2013, 373, 59−63.

(48) Byres, M.; Cox, P. J.; Kay, G.; Nixon, E. CrystEngComm 2009, 11, 135−142.

.

Legends to figures

Figure 1 Zafirlukast (ZF).

Figure 2. PXRD of the new solvates and anhydrous form of ZF.

Figure 3 DSC and TGA of the ZF ACN solvate. DSC curve of the anhydrous form is shown for comparison.

Fig. 4 DSC and TGA of the ZF BuOH solvate. DSC curve of the anhydrous form is shown for comparison.

Figure 5. Ribbons of self-assembled molecules of ZF in Form X.

Figure 6. (a) Cmethoxy−H···π interaction and (b) Carene−H···π interaction in Form X of ZF.

Figure 7. Self-assembled dimers of ZF stabilized by peripheral acetonitrile−amide interactions in ZF acetonitrile solvate (some hydrogens have been omitted for clarity).

Figure 8. Hydrogen bond interactions established between butanol and ZF molecules in the butanol solvate.

Figure 9. Chains of hydrogen-bonded molecules of ZF in the butanol solvate.

Figure 10. CH···π interactions observed in the butanol solvate.

Figure 11. Chains of ZF molecules in the piperazine cocrystal.

Figure 12. Cavity occupied by the piperazine molecule in the cocrystal (hydrogens and fragments of the ZF molecules have been omitted for clarity).

Figure 13. PXRD patterns of the five ZF/piperazine cocrystals.

Figure 14. PXRD patterns of the two 2:1 ZF/piperazine cocrystals.

Figure 15. Le Bail fit of 2:1 ZF/piperazine cocrystal Form B.

Figure 16. DSC and TGA traces of the 1:1 cocrystal Form C.

FIGURE 1

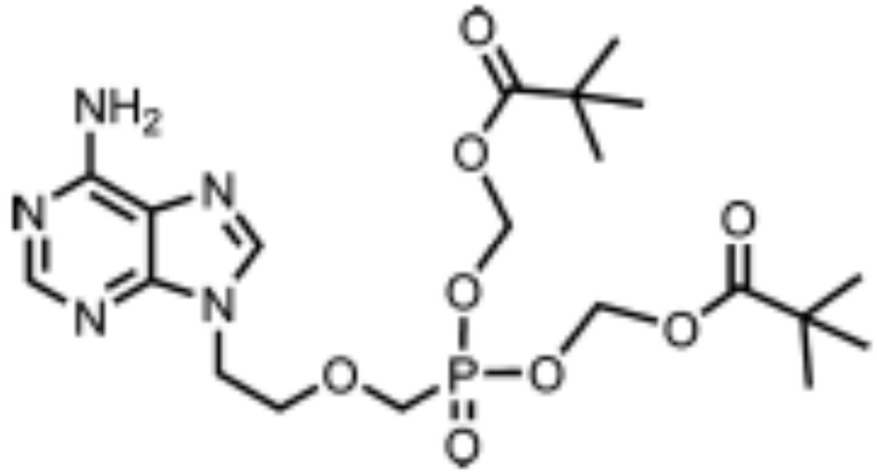

FIGURE 2

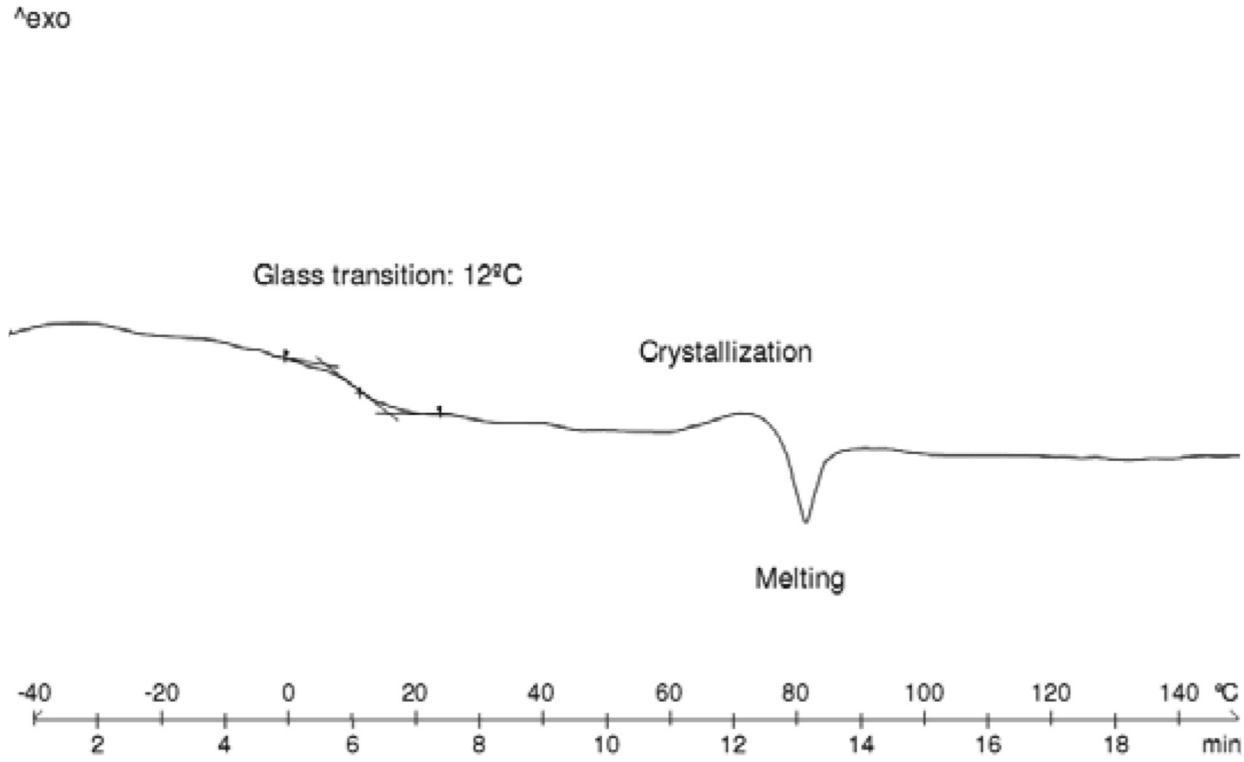
^exo
Glass transition: 12ºC
Crystallization
Melting
-40
-20
0
20
40
60
80
100
120
140 ºC
2
4
6
8
10
12
14
16
18
min

458 **FIGURE 3**

459

460

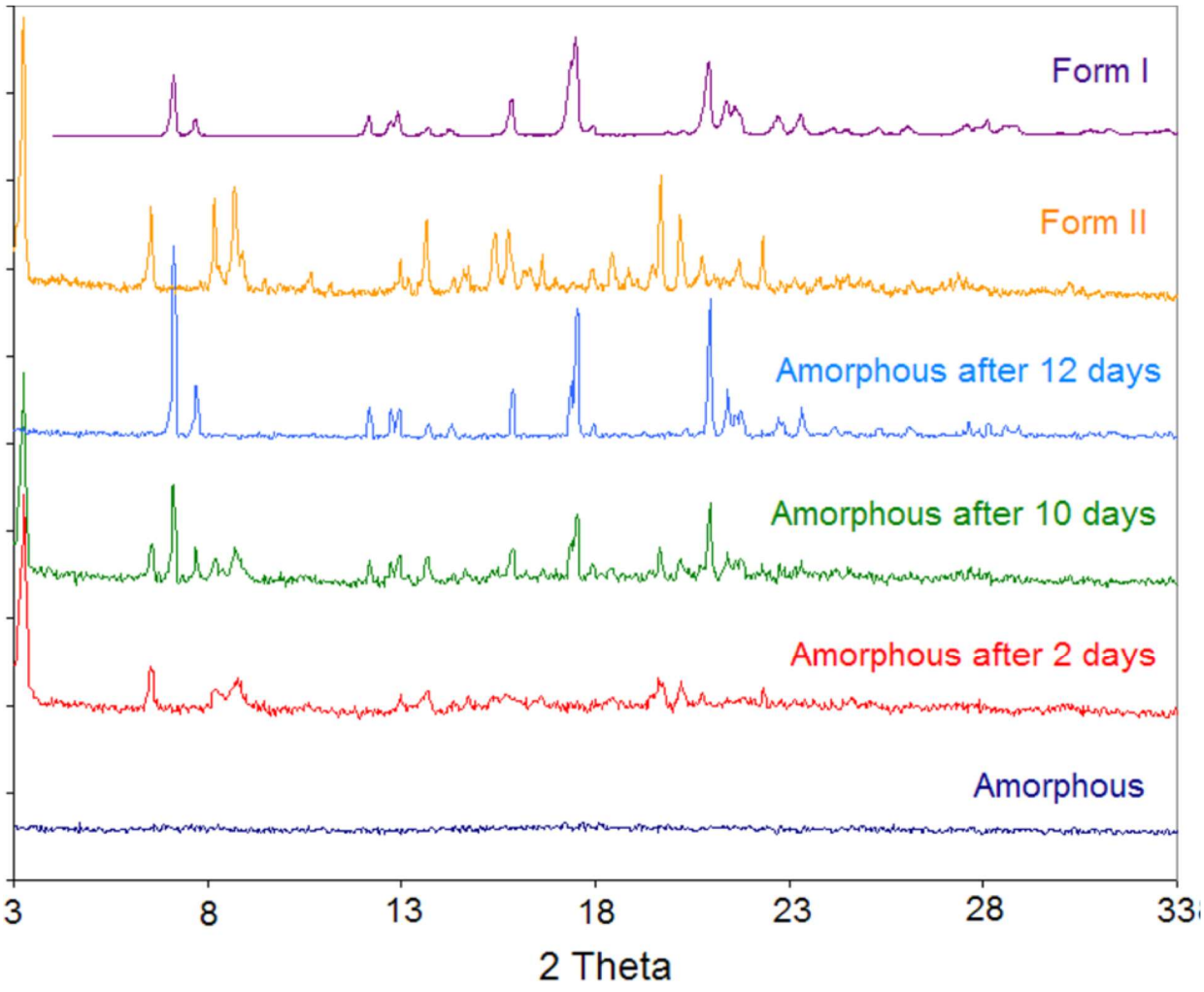

461

462

463

464

FIGURE 4

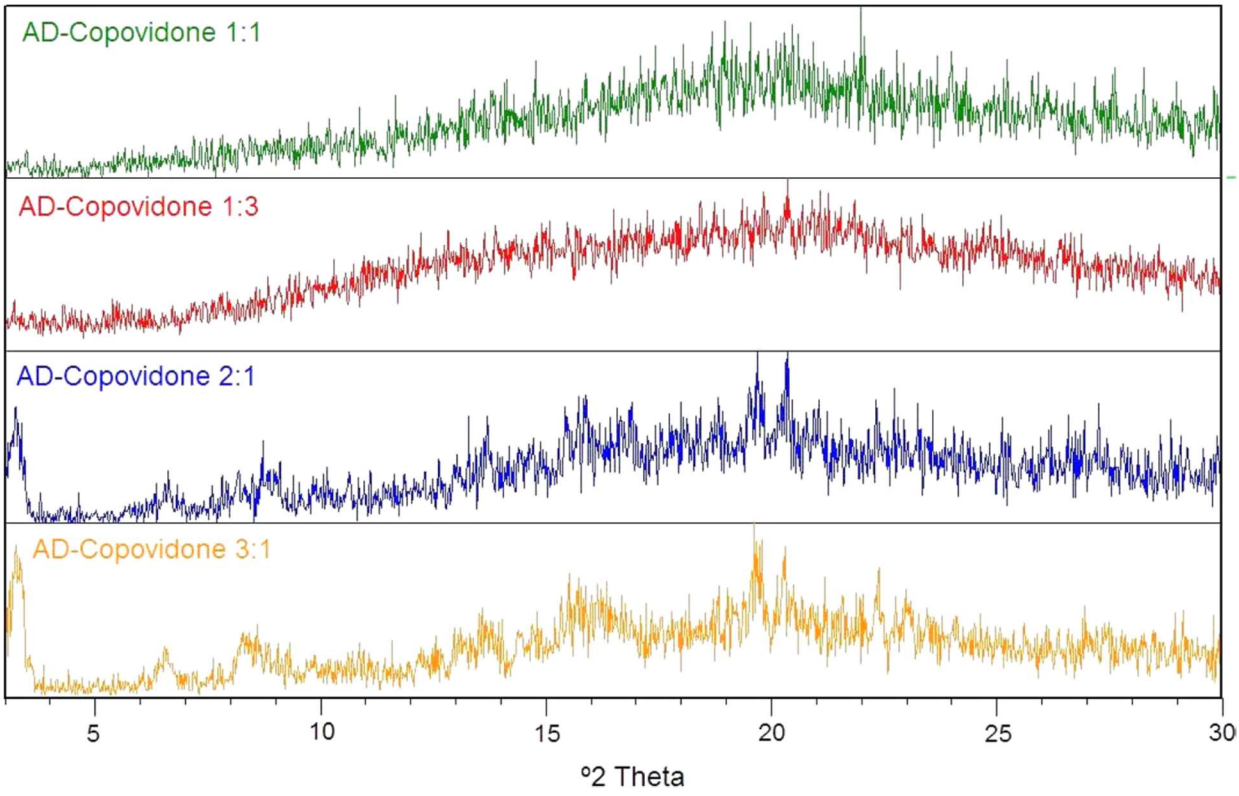
AD-Copovidone 1:1
AD-Copovidone 1:3
AD-Copovidone 2:1
AD-Copovidone 3:1
5
10
15
20
25
30
°2 Theta

FIGURE 5

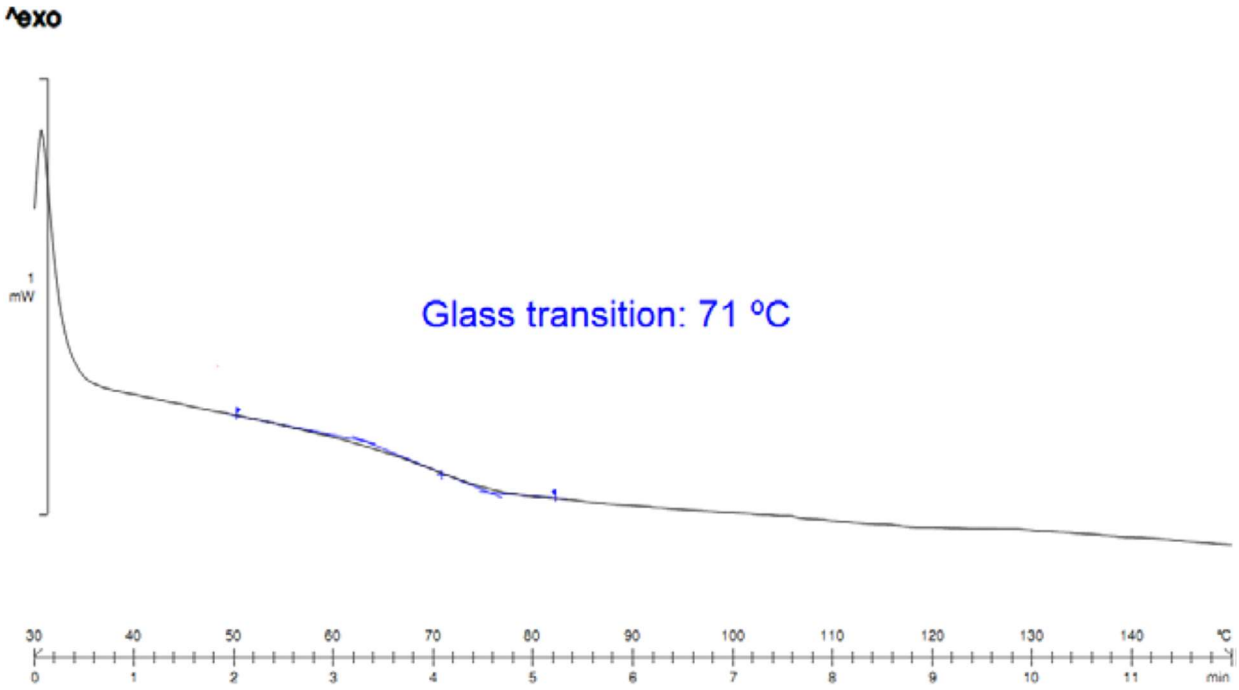
^exo
1
mW
Glass transition: 71 °C
30
40
50
60
70
80
90
100
110
120
130
140
°C
0
1
2
3
4
5
6
7
8
9
10
11
min

FIGURE 6

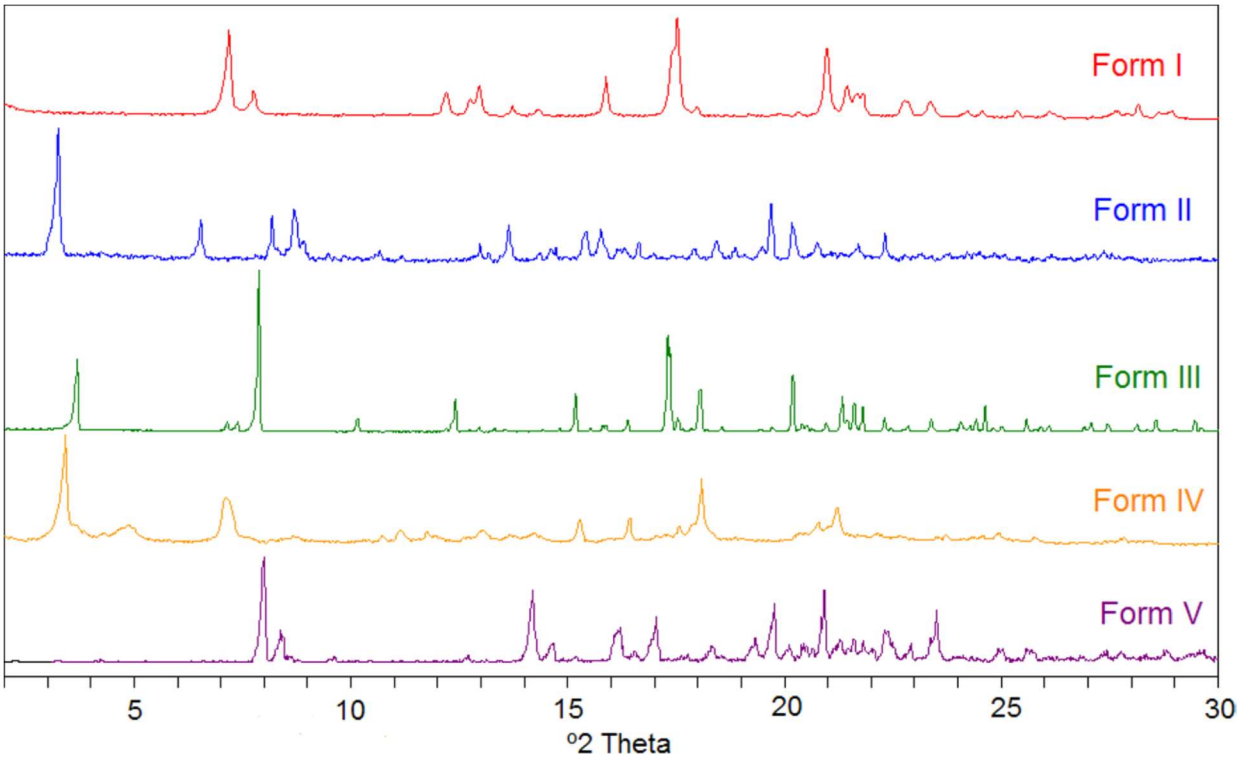

FIGURE 7

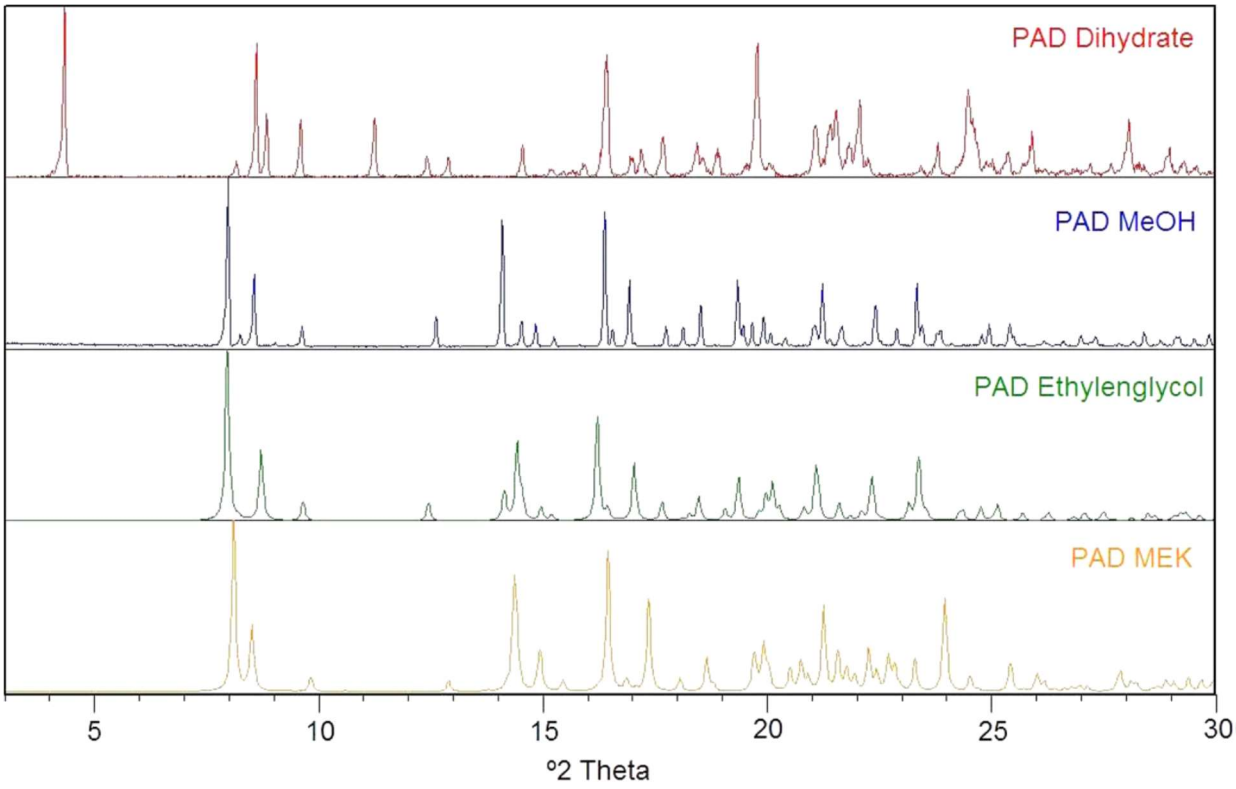
PAD Dihydrate
PAD MeOH
PAD Ethylenglycol
PAD MEK
5
10
15
20
25
30
º2 Theta

FIGURE 8

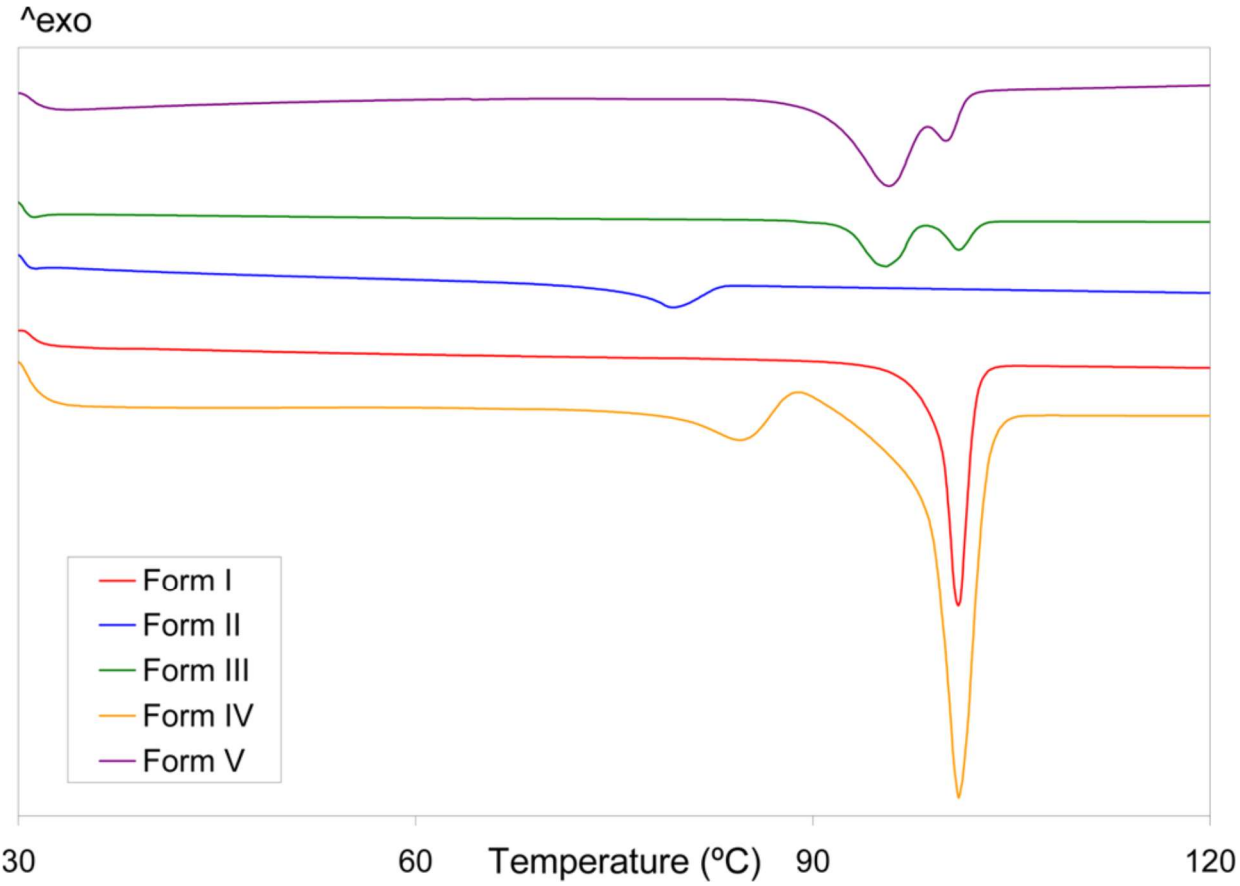
^exo
Form I
Form II
Form III
Form IV
Form V
30
60
Temperature (°C)
90
120

FIGURE 9

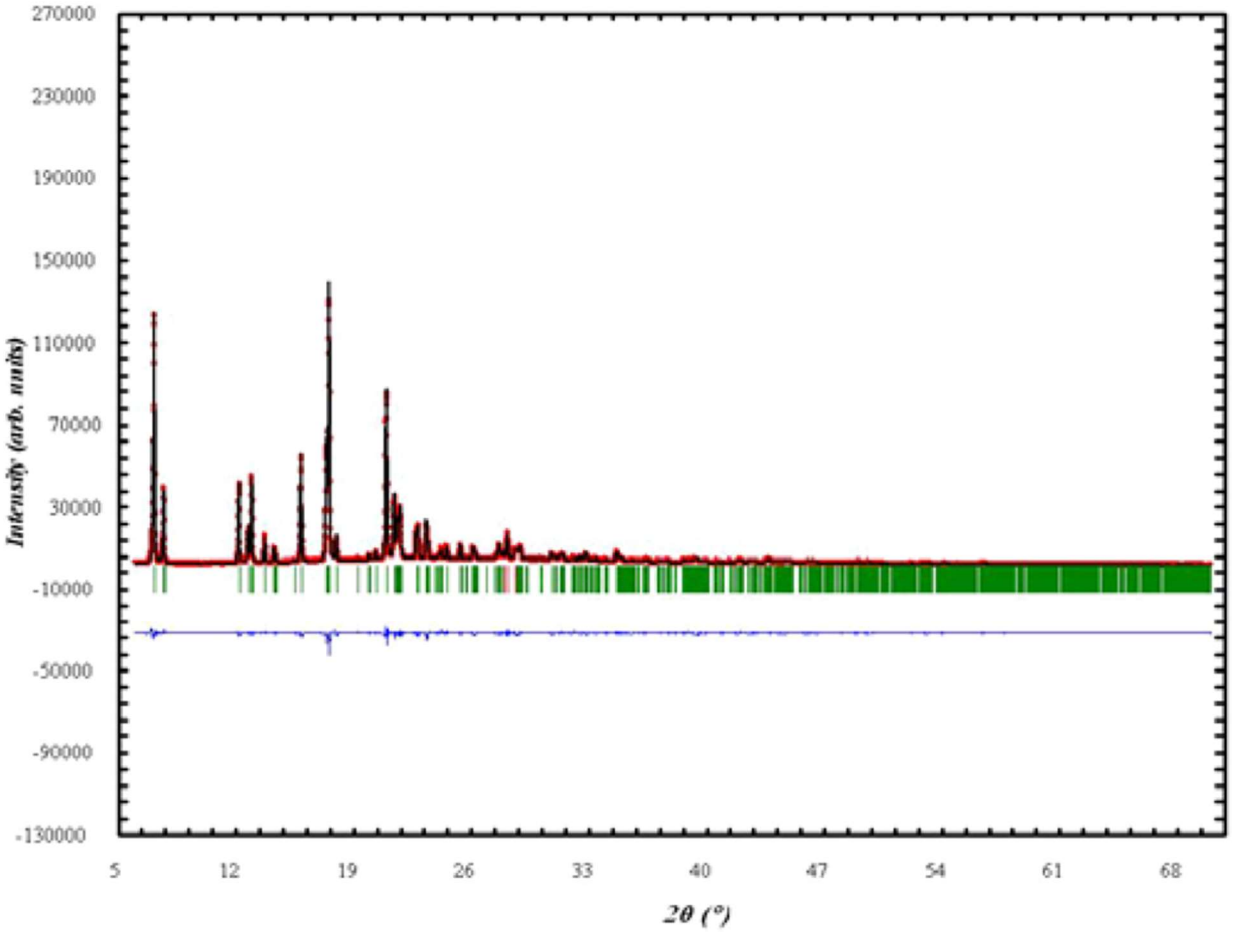
270000
230000
190000
150000
110000
70000
30000
-10000
-50000
-90000
-130000
Intensity (arb. units)
5
12
19
26
33
40
47
54
61
68
2θ (°)

FIGURE 10

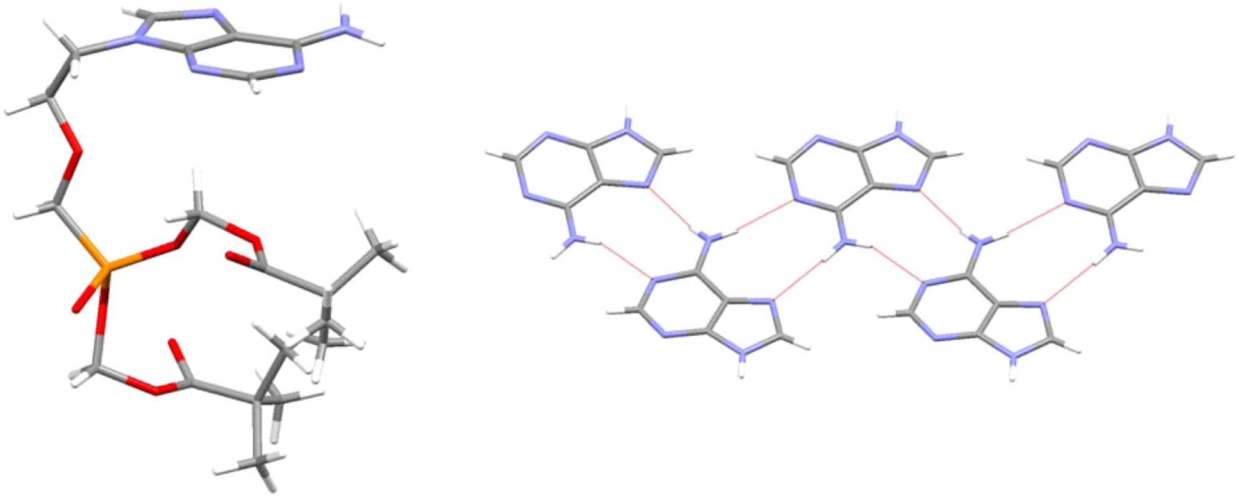

(a) (b)

FIGURE 11

FIGURE 12

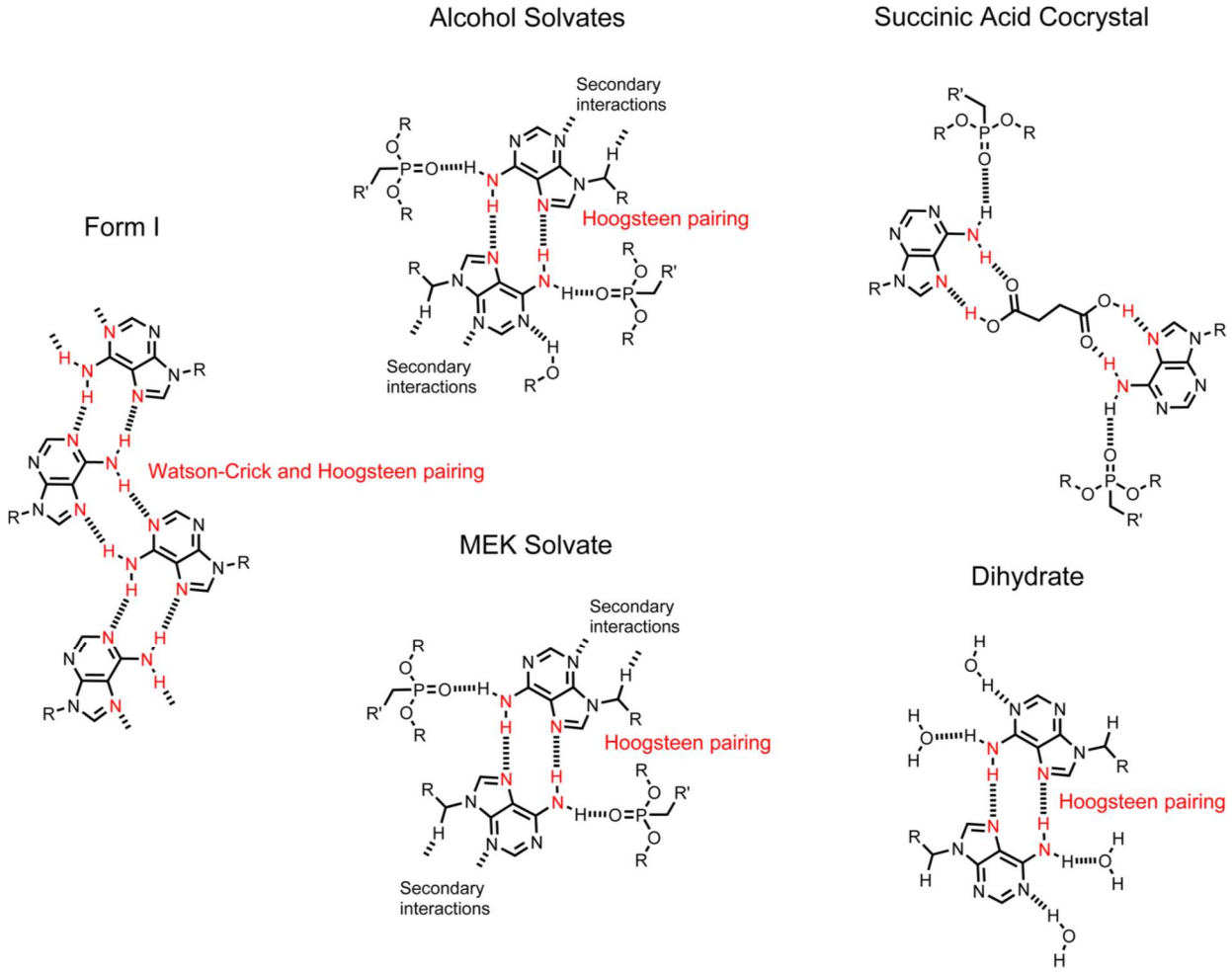
Alcohol Solvates
Succinic Acid Cocrystal
Secondary interactions
Hoogsteen pairing
Form I
Watson-Crick and Hoogsteen pairing
Secondary interactions
MEK Solvate
Dihydrate
Secondary interactions
Hoogsteen pairing
Secondary interactions
Hoogsteen pairing

513 **Table 1.** Physicochemical Data Obtained from DSC Analyses (100 °C/min, He)a

514

form	melting point (°C)	enthalpy of fusion (J/g)
I	98	78
II	78	51
III	93	73
IV	80	56
V	91	66

[a]Results are the average of three measurements.

515

516

517

518

519

Table 2. Crystal Data and Structure Refinement Parameters for the Different Forms of AD

structure	Form 1	methanol solvate	ethylenglycol hemisolvate	MEK hemisolvate
empirical formula	$C_{20}H_{23}N_3O_3P$	$C_{20}H_{23}N_3O_3P \cdot CH_4O$	$(C_{20}H_{22}N_3O_3P)0.5(C_2H_6O_2)$	$2(C_{20}H_{23}N_3O_3P)C_4H_8O$
formula weight	501.48	533.52	532.51	1075.05
temperature (K)	293	293(2)	293(2)	117(2)
wavelength (Å)	1.54180	0.71073	0.71073	0.71073
crystal system	monoclinic	triclinic	triclinic	triclinic
space group	C_c	$P\bar{1}$	$P\bar{1}$	$P\bar{1}$
a, b, c (Å)	13.1287(1), 24.6784(3), 8.34752(8)	10.568(6), 12.031(5), 13.327(5)	10.555(7), 12.005(7), 13.366(6)	10.3496(5), 12.0188(6), 12.9829(6)
α, β, γ (deg)	90, 100.6575(5), 90	116.71(2), 105.63(3), 96.82(3)	108.71(3), 113.68(3), 98.42(4)	115.175(2), 105.644(2), 98.228(2)
volume (Å^3)	2657.91(5)	1399.9(11)	1393.1(14)	1344.40(11)
Z, density (calc) (Mg/m^3)	4, 1.253	2, 1.266	2, 1.269	1, 1.328
absorption coefficient (mm^{-1})		0.152	0.153	0.158
$F(000)$	1064.0	568	566	572
crystal size (mm^3)		0.2 × 0.1 × 0.1	0.2 × 0.1 × 0.1	0.600 × 0.310 × 0.250
θ range for data collection (deg)	5.0−39.9	2.73−32.37	2.78−32.38	2.14−33.98
limiting indices		$-14 \le h \le 14, -18 \le k \le 17, -17 \le l \le 20$	$-15 \le h \le 15, -17 \le k \le 17, -16 \le l \le 20$	$-16 \le h \le 15, -18 \le k \le 16, 0 \le l \le 19$
reflections collected/unique		13925/7227 [R(int) = 0.0412]	15052/7961 [R(int) = 0.0499]	9164/9164 [R(int) = 0.0000]
completeness to θ (%)		93.7	93.7	99.9
absorption correction		empirical	empirical	semiempirical from equivalents
max and min transmission		0.99 and 0.98	0.98 and 0.97	0.961 and 0.943
refinement method	Rietveld	full-matrix least-squares on F^2	full-matrix least-squares on F^2	full-matrix least-squares on F^2
data/parameters	1410/186/162	7227/6/383	7961/5/388	9164/9/335
goodness-of-fit on F^2	12.7	1.093	1.100	1.074
final R indices [$I > 2\sigma(I)$]		$R_1 = 0.0554$, $wR_2 = 0.1504$	$R_1 = 0.0629$, $wR_2 = 0.1542$	$R_1 = 0.0399$, $wR_2 = 0.1057$
R indices (all data)	$R_1 = 0.0384$, $wR_2 = 0.0513$	$R_1 = 0.0707$, $wR_2 = 0.1601$	$R_1 = 0.1114$, $wR_2 = 0.1717$	$R_1 = 0.0469$, $wR_2 = 0.1101$
largest diff peak and hole (e Å^{-3})		0.324 and −0.248	0.292 and −0.255	1.392 and −1.244
CCDC	964906	1027663	1027664	1027665